PASJ: Publ. Astron. Soc. Japan **60**, 183–190, 2008 April 25

VLBI Observations of Water Masers in Onsala 1: Massive Binary Star-Forming Site?

Takumi NAGAYAMA
Graduate School of Science and Engineering, Kagoshima University, 1-21-35 Kôrimoto, Kagoshima, Kagoshima 890-0065
and
Akiharu NAKAGAWA, Hiroshi IMAI, Toshihiro OMODAKA, andYoshiaki SOFUE
Faculty of Science, Kagoshima University, 1-21-35 Kôrimoto, Kagoshima, Kagoshima 890-0065
nagayama@astro.sci.kagoshima-u.ac.jp

(Received 2007 September 4; accepted 2007 November 8)

Abstract

We present the proper motions of water masers toward the Onsala 1 star-forming region, observed with the Japanese VLBI network at three epochs spanning 290 days. We found that there are two water-maser clusters (WMC 1 and WMC 2) separated from each other by $1\farcs6$ (2900 AU at a distance of 1.8 kpc). A proper-motion measurement revealed that WMC 1 is associated with a bipolar outflow elongated in the east–west direction with an expansion velocity of $69 \pm 11\,\mathrm{km\,s^{-1}}$. WMC 1 and WMC 2 are associated with two 345 GHz continuum dust emission sources, which are located $2''$ (3600 AU) east from the core of an ultracompact H II region traced by 8.4 GHz radio continuum emission. This indicates that the star-formation activity of Onsala 1 could move from the west side of the ultracompact H II region to the east side of two young stellar objects associated with the water masers. We have also found that the WMC 1 and UC H II regions could be gravitationally bound. Their relative velocity along the line of sight is $\sim 3\,\mathrm{km\,s^{-1}}$, and the total mass is $\sim 37 M_{\odot}$. Onsala 1 seems to harbor a binary star at a different evolutionary stage.

Key words: ISM: H II region — ISM: individual (Onsala 1) — masers — stars: formation — VLBI

1. Introduction

Star-forming regions are often associated with water-maser emissions, and Very Long Baseline Interferometry (VLBI) monitoring observations of the water maser provide a unique tool to study the structure and kinematics of a star-forming region. Analyses of spatial positions, Doppler velocities, and proper motions of water masers have often revealed the 3-D gas kinematics in the vicinity of young stellar objects (YSOs) (e.g., Orion-KL: Genzel et al. 1981; Cepheus A: Torrelles et al. 2001; G192.16–3.84: Imai et al. 2006; G24.78+0.08: Moscadelli et al. 2007).

The Onsala 1 star-forming region (hereafter ON 1) has an ultracompact (UC) H II region observed in radio continuum emissions at 8.4 GHz and 23.7 GHz (Zheng et al. 1985; Argon et al. 2000). The centimeter radio continuum luminosity of this UC H II region is $10^{4.2} L_{\odot}$, which indicates an exciting star of the ZAMS type B0 (MacLeod et al. 1998). Kumar et al. (2004) reported the presence of multiple outflows from the UC H II region. One outflow traced by the ^{12}CO $J = 2$–1 line is elongated in the east–west direction with a velocity of $12\,\mathrm{km\,s^{-1}}$ (respect to the systemic velocity of ON 1 $V_{\mathrm{LSR}} = 12\,\mathrm{km\,s^{-1}}$), and other possible outflow traced by the H^{13}CO^{+} $J = 1$–0 line is elongated in the northeast–southwest direction with a velocity of $4.5\,\mathrm{km\,s^{-1}}$ (Kumar et al. 2004). The H^{13}CO^{+} outflow is, however, on the other hand, interpreted as being a rotating disk by observations in the NH_3 and the same H^{13}CO^{+} lines (Zheng et al. 1985; Lim et al. 2002). These molecular line observations suggest that there are several YSOs in or around the UC H II region of ON 1.

Submillimeter continuum emission at 345 GHz (0.85 mm) using the Submillimeter Array (SMA) have resolved two components separated in the northeast–southwest direction (Su et al. 2004). The 345 GHz continuum emissions are elongated in the east side of the UC H II region. It is known that YSOs at the youngest stage often show a spectral energy distribution with the peak flux at submillimeter wavelength, originating from the dust envelopes (André et al. 1993). The strong submillimeter emissions from these two sources would, therefore, indicate that they are the youngest YSOs contained in ON 1. Thus, YSOs at different evolutionary stages seem to be found in ON 1.

A VLBI observation of the water masers (Downes et al. 1979) shows that ON 1 has two clusters of water masers separated by $\sim 2''$ (3600 AU at our assumed distance of 1.8 kpc) in the northeast–southwest direction. These two clusters appear to have offsets from the core of the UC H II region traced by 23.7 GHz continuum emission (Zheng et al. 1985). This fact suggests that the water masers are associated with newly YSOs that formed around the UC H II region. In order to confirm this, new multi-epoch VLBI observations to measure the proper motions of water masers are necessary.

The VLBI observation of Downes et al. (1979) detected water masers at $V_{\mathrm{LSR}} = 5$–$23\,\mathrm{km\,s^{-1}}$. Kurtz and Hofner (2005) found that the water-maser emission of ON 1 has a larger velocity range ($V_{\mathrm{LSR}} = -53$ to $63\,\mathrm{km\,s^{-1}}$), and suggested that these high-velocity components would give important information about other star-formation signposts in ON 1.

Here, we present the distribution and proper motions of 22.2 GHz water masers towards ON 1. Section 2 describes

Table 1. Status of the telescopes, data reduction, and resulting performances in the individual epochs of the JVN observations.

Epoch	Date	Duration (hr)	Used telescopes*	Reference velocity† ($\mathrm{km\,s^{-1}}$)	1-σ level noise ($\mathrm{Jy\,beam^{-1}}$)	Synthesized beam‡ (mas)	Number of detected features
1 ...	2005 Mar 24	10	MZ, IR, OG, IS, KS§, NB	16.5	0.045	1.9×0.7, -38°	21
2 ...	2005 Jun 1	10	MZ, OG, IS, KS, NB	16.5	0.032	3.4×1.3, -86°	18
3 ...	2006 Jan 8	10	MZ, IR, OG, IS, KS	16.5	0.039	1.7×0.9, -51°	23

* Telescopes that were effectively operated and whose recorded data were valid: MZ: the VERA 20-m telescope at Mizusawa, IR: the VERA 20-m telescope at Iriki, OG: the VERA 20-m telescope at Ogasawara Is, IS: the VERA 20-m telescope at Ishigakijima Is, KS: the NiCT 34-m telescope at Kashima, NB: the NRO 45-m telescope at Nobeyama.
† Local-standard-of-rest velocity of the spectral channel used for the phase reference in data reduction.
‡ The synthesized beam made in natural weight; major and minor axis lengths and position angle.
§ Ceasing operation for 8 hours due to strong winds.

observations with the Japanese VLBI network (JVN, e.g., Doi et al. 2006; Imai et al. 2006) and data reduction. Section 3 shows the distribution and proper motion of the water masers. Section 4 discusses the driving sources of water masers and the structure of ON 1 through comparisons with previous observations. Although the distance to ON 1 is uncertain, a near kinematic distance of 1.8 kpc is favored by most authors (e.g., MacLeod et al. 1998; Kumar et al. 2004). We therefore adopt a distance of 1.8 kpc to this source.

2. Observations

The VLBI observations of ON 1 were made on 2005 March 24, and June 1, and on 2006 January 8 using five or six telescopes of the JVN composed of four 20-m telescopes of the VLBI Exploration of Radio Astrometry (VERA) of the National Astronomical Observatory of Japan (NAOJ), a 45-m telescope of the Nobeyama Radio Observatory (NRO), and a 34-m telescope of the National institute of Information and Communications Technology (NiCT) at Kashima. ON 1 and a calibrator source (ICRF J192559.6+210626) for clock parameter corrections were observed for 10 hours in total per observing epoch. Left-hand circular polarization signals were recorded with a SONY DIR1000 recorder at a data rate of 128 Mbps and in two base band channels with a band width of 16 MHz each, covering a radial velocity span of $215.7\,\mathrm{km\,s^{-1}}$. A data correlation was made with the Mitaka FX correlator (Chikada et al. 1991). The correlation outputs consisted of 1024 velocity channels, yielding frequency and velocity resolutions of 15.625 kHz and $0.21\,\mathrm{km\,s^{-1}}$, respectively.

Data reduction was performed using the Astronomical Image Processing System (AIPS) of National Radio Astronomy Observatory (NRAO). Calibrations of the clock parameters, bandpass characteristics, visibility amplitudes, and visibility phases as well as velocity tracking were carried out in a standard manner. The clock parameters (clock offset and clock rate offset) were calibrated using the residual delay and delay rate for a calibrator source which was observed every hour. A bandpass calibration was made using auto-correlation spectra of the continuum source. The amplitude calibration was made using the system noise temperatures; they were evaluated using the "R-Sky" method, by observing a reference black body at the beginning of each scan (typically every hour). The observed frequencies of the maser lines were converted to the local-standard-of-rest (LSR) velocities using a rest frequency of 22.235080 GHz for the H_2O 6_{16}–5_{23} transition. For phase calibrations, the visibilities of all velocity channels were phase-referenced to the reference maser spot at a LSR velocity of $16.5\,\mathrm{km\,s^{-1}}$, which is one of the brightest spots that exhibits no sign of structure according to the closure phase deviation from zero. A typical size of the synthesized beam was ~ 1 milliarcsecond (mas) in the three observations (see table 1).

We identified all emission components stronger than 7-times the rms noise level in the images for each spectral channel. The identification of a water-maser feature, which represents a physical feature and consisting of a cluster of maser spots or velocity components, was made by the procedure shown in several previous papers (e.g., Imai et al. 2000). We identified it as a feature consisting of spots within a beam size of approximately 1 mas (1.8 AU). The feature position is defined as a brightness peak in the feature. Position uncertainties for the features were typically 0.05 mas. We detected 21, 18, and 23 maser features in three epochs, respectively.

3. Results

3.1. *Water Maser Spectrum*

Figure 1 shows the total power spectra of the ON 1 water masers obtained with the Nobeyama 45-m and Mizusawa 20-m telescopes. There are low-velocity components ($V_{\mathrm{LSR}} \simeq$ 4–$22\,\mathrm{km\,s^{-1}}$) near the systemic velocity of ON 1 observed in the NH_3 line ($V_{\mathrm{LSR}} =$ 10–$12\,\mathrm{km\,s^{-1}}$: Zheng et al. 1985) and, in addition, high-velocity blue-shifted ($V_{\mathrm{LSR}} \simeq -60$ to $-20\,\mathrm{km\,s^{-1}}$), and red-shifted ($V_{\mathrm{LSR}} \simeq$ 50–$60\,\mathrm{km\,s^{-1}}$) components. The blue- and red-shifted components symmetrically appear around the systemic velocity. We have detected most of the velocity components seen in the previous observations (Downes et al. 1979; Kurtz & Hofner 2005).

The peak flux density of the low-velocity components is typically 100 Jy, and does not change from epoch to epoch. On the other hand, the fluxes of the high-velocity components are time-variable. The blue-shifted components had 8 Jy in 2005 March, and increased to more than 150 Jy in 2006 January. These blue-shifted components were already found about 30 years ago by a single-dish observation (Genzel & Downes 1977). However, they were too weak to be mapped by the VLBI in 1977 (Downes et al. 1979). The red-shifted

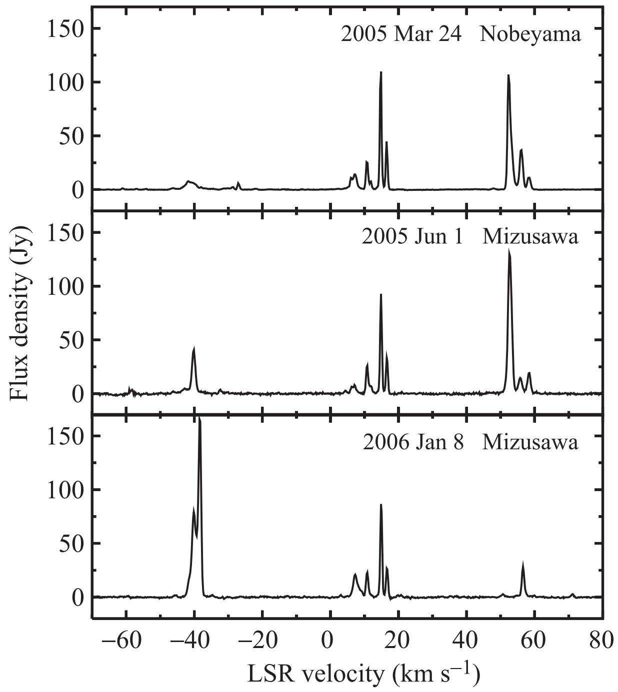

Fig. 1. Spectra of the total flux of ON 1 water masers, obtained in three epochs with the Nobeyama 45-m and the Mizusawa 20-m telescopes The velocity resolution is equal to a channel width of 0.21 km s^{-1}.

components were strong (approximately 100–150 Jy) during our first and second VLBI observations (2005 March–June). However, they decreased to 30 Jy in 2006 January. These redshifted components were not detected in 1977 and 1987 (Genzel & Downes 1977; Cesaroni et al. 1988), and detected for the first time in 1995 (Kurtz & Hofner 2005).

The statistics of water masers show that high-velocity components are generally highly variable, and are as weak as 0.1–10% of the low-velocity component (Genzel & Downes 1977). Similarly, the high-velocity component in ON 1 is also highly variable. However, the high-velocity component is sometimes stronger than the low-velocity component. Its intensity is 10–200% of the low-velocity component.

3.2. *Water Maser Distributions*

Figure 2 shows the distributions and the proper-motion vectors of water masers in ON 1 (for proper motions, see next subsection). Twenty one of the features detected at the first epoch are plotted. The color index denotes the LSR velocity range from -41.8 to $58.4\,\mathrm{km\,s^{-1}}$, where the 21 features are located. The map origin is located at the position of the reference maser feature at $V_{\mathrm{LSR}} = 16.5\,\mathrm{km\,s^{-1}}$, which is estimated to be $\alpha(\mathrm{J2000}) = 20^{\mathrm{h}}10^{\mathrm{m}}09\overset{\mathrm{s}}{.}201 \pm 0\overset{\mathrm{s}}{.}004$ and $\delta(\mathrm{J2000}) = 31^{\circ}31'36\overset{''}{.}02 \pm 0\overset{''}{.}08$ from a fringe rate analysis. ON 1 has two clusters of water maser features located at $(X, Y) \simeq (0'', 0'')$ (hereafter WMC 1 = water-maser cluster 1) and at $(X, Y) \simeq (-0\overset{''}{.}9, -1\overset{''}{.}4)$ (hereafter WMC 2). The separation of WMC 1 and WMC 2 is $1\overset{''}{.}6$, which corresponds to 2900 AU.

WMC 1 is distributed within a region of $\sim 320 \times 50$ mas (580×90 AU). The blue- ($V_{\mathrm{LSR}} = -41.8$ to $-28.5\,\mathrm{km\,s^{-1}}$) and red-shifted ($V_{\mathrm{LSR}} = 52.4$–$58.4\,\mathrm{km\,s^{-1}}$) maser features appeared in WMC 1. Their separation is 195 mas, which corresponds to 350 AU. The blue- and red-shifted maser features are distributed within areas of 9×11 mas (16×20 AU) and 5×14 mas (9×25 AU), respectively, and were not detected outside of these regions. The systemic velocity of WMC 1 is $V_{\mathrm{LSR}} = 9.3 \pm 6.8\,\mathrm{km\,s^{-1}}$, derived from three mean velocities of blue-shifted ($V_{\mathrm{LSR}} = -40.5 \pm 4.3\,\mathrm{km\,s^{-1}}$), red-shifted ($V_{\mathrm{LSR}} = 55.4 \pm 2.0\,\mathrm{km\,s^{-1}}$), and low-velocity ($V_{\mathrm{LSR}} = 13.1 \pm 3.2\,\mathrm{km\,s^{-1}}$) features detected in three epoch observations.

WMC 2 is distributed within a region of $\sim 160 \times 380$ mas (290×680 AU). Only the low-velocity features ($V_{\mathrm{LSR}} = 7.2$–$14.8\,\mathrm{km\,s^{-1}}$) were detected in WMC 2. The systemic velocity of WMC 2 is derived to be $V_{\mathrm{LSR}} = 11.3 \pm 2.3\,\mathrm{km\,s^{-1}}$ from the mean velocity of low-velocity features detected in three epoch observations.

3.3. *Proper Motions*

Table 2 lists the observed proper motions of 14 maser features in ON 1. The maser features in different epochs were identified as the *same* feature, if their LSR velocities were equal to each other within $0.42\,\mathrm{km\,s^{-1}}$ (2-channel), and if their positions were coincident within 2.5 mas at the first to second epochs and 7 mas at the second to third epochs. The spatial ranges of 2.5 and 7 mas correspond to a proper motion of $100\,\mathrm{km\,s^{-1}}$ ($12\,\mathrm{mas\,yr^{-1}}$). Based on these identification criteria, each maser feature was identified in at least two epochs. The proper motions were calculated by performing a linear least-squares fit of the positional offsets to the elapsed time. Figure 3 shows the observed time variations of right ascension and declination offsets (relative to feature "5") of five features detected at all three epochs.

The proper motions of WMC 1 exhibit a bipolar outflow structure in the east–west direction. The proper motions show high ($69 \pm 11\,\mathrm{km\,s^{-1}}$) and low ($\sim 10\,\mathrm{km\,s^{-1}}$) expansion velocities. The blue- and red-shifted features represent the high-velocity and collimated outflow. For the blueshifted features, the proper motion of the brightest feature at $V_{\mathrm{LSR}} = -40.5\,\mathrm{km\,s^{-1}}$ was obtained to be $(\mu_x, \mu_y) = (7.9, -3.3)\,\mathrm{mas\,yr^{-1}}$, which corresponds to $(V_x, V_y) = (68, -28)\,\mathrm{km\,s^{-1}}$. The mean proper motion of four redshifted features ($V_{\mathrm{LSR}} = 52.4$–$58.4\,\mathrm{km\,s^{-1}}$) is $(\mu_x, \mu_y) = (-3.0 \pm 0.7, 0.4 \pm 0.2)\,\mathrm{mas\,yr^{-1}}$, which corresponds to $(V_x, V_y) = (-25 \pm 6, 3 \pm 2)\,\mathrm{km\,s^{-1}}$. These proper motions appear to be associated with a common origin.

The simplest explanation for this fact is that the water masers in WMC 1 are associated with a bipolar outflow which is ejected from a YSO located at the midpoint of the blue- and red-shifted features. The expansion velocity between the blue- and red-shifted features was estimated to be $69 \pm 11\,\mathrm{km\,s^{-1}}$, from the differences of their proper motions $(\Delta V_x, \Delta V_y) = (93 \pm 6, 31 \pm 2)\,\mathrm{km\,s^{-1}}$ and LSR velocities $\Delta V_{\mathrm{LSR}} = 95 \pm 3\,\mathrm{km\,s^{-1}}$. The inclination angle of the direction of expansion was determined to be $44^{\circ} \pm 3^{\circ}$. The position angle and opening angle derived from the distributions of blue- and red-shifted features are 92° and 10°, respectively. The LSR velocities of three low-velocity features ($V_{\mathrm{LSR}} = 12.1$, 15.0, $15.6\,\mathrm{km\,s^{-1}}$) in WMC 1 show a low expansion velocity

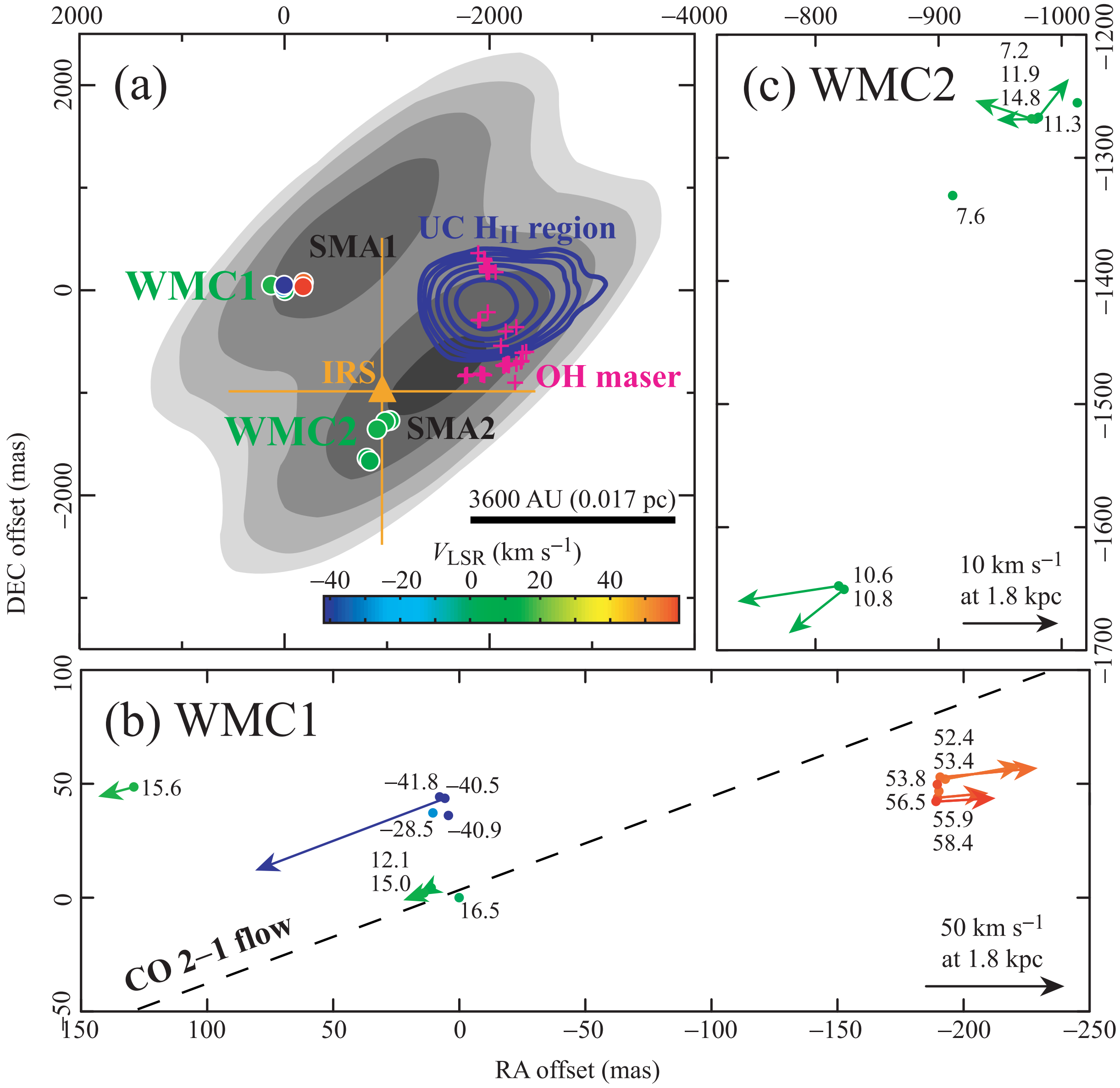

Fig. 2. (a) Observed water maser distributions (colored filled circle) superimposed on an 8.4 GHz radio continuum map (thick contour) of the UC H II region (Argon et al. 2000). The gray-scale map shows the 345 GHz radio continuum exhibiting dust emission (Su et al. 2004), where the lowest gray contour indicates half of the peak brightness. The crosses show the OH maser distribution (Fish et al. 2005) and the triangle indicates the 10 μm infrared source (Kumar et al. 2003). The map origin with RA and DEC offsets = (0, 0) is at α (J2000) = $20^{\rm h}10^{\rm m}09.^{\rm s}201 \pm 0.^{\rm s}004$ and δ (J2000) = $31^\circ 31' 36.''02 \pm 0.''08$. 1000 mas corresponds to 1800 AU at a distance of 1.8 kpc. (b), (c) Close-up to the two water-maser clusters (WMC 1 and WMC 2) with proper-motion vectors. The colored arrows and number added for each feature denote the LSR velocity. The arrows at the bottom-right corner in (b) and (c) indicate proper motions of 5.9 mas yr^{-1} and 1.2 mas yr^{-1} (50 km s^{-1} and 10 km s^{-1}), respectively. The dashed line in (b) indicates the axis of the bipolar outflow observed in the ^{12}CO $J = 2$–1 line (Kumar et al. 2004)

Table 2. Parameters of the water-maser features identified by proper motion toward ON 1.

ID*	Offset† (mas)				LSR velocity (km s^{-1})	Proper motion† (mas yr^{-1})				Peak intensity at three epochs (Jy beam^{-1})		
	X	σX	Y	σY	$V_{\rm LSR}$	μ_x	$\sigma\mu_x$	μ_y	$\sigma\mu_y$	Epoch 1	Epoch 2	Epoch 3
1	129.04	0.05	48.58	0.05	15.69	1.49	...	−0.44	...	0.40	...	0.65
2	13.99	0.01	1.98	0.02	15.06	0.86	0.15	−0.33	0.05	13.70	15.00	21.50
3	11.04	0.03	4.29	0.03	12.11	0.57	0.03	−0.34	0.13	1.03	0.81	0.56
4	5.69	0.06	43.55	0.08	−40.54	7.93	...	−3.33	...	0.53	6.82	...
5	0.00	0.06	0.00	0.04	16.53	0.00	...	0.00	...	6.55	6.75	5.28
6	−189.05	0.02	42.17	0.02	58.45	−2.48	...	0.15	...	3.09	5.50	...
7	−189.71	0.02	43.91	0.02	55.93	−2.11	...	0.21	...	7.53	3.69	...
8	−190.73	0.01	52.90	0.01	53.40	−4.07	...	0.42	...	10.60	17.90	...
9	−192.73	0.01	52.05	0.01	52.56	−3.22	...	0.63	...	28.00	26.00	...
10	−818.83	0.13	−1647.78	0.07	10.64	1.73	...	−0.26	...	...	1.63	1.90
11	−823.19	0.03	−1650.52	0.02	10.85	0.94	0.16	−0.75	0.04	2.96	2.67	3.69
12	−975.58	0.07	−1268.37	0.06	14.85	0.96	...	0.31	...	1.31	...	0.66
13	−978.89	0.04	−1268.50	0.04	11.90	0.66	0.20	−0.01	0.03	0.89	1.16	0.71
14	−981.02	0.04	−1267.26	0.03	7.27	−0.52	0.11	0.66	0.00	2.23	1.30	0.86

* Feature ID number.
† Relative value with respect to the position-reference maser feature: ID 5.

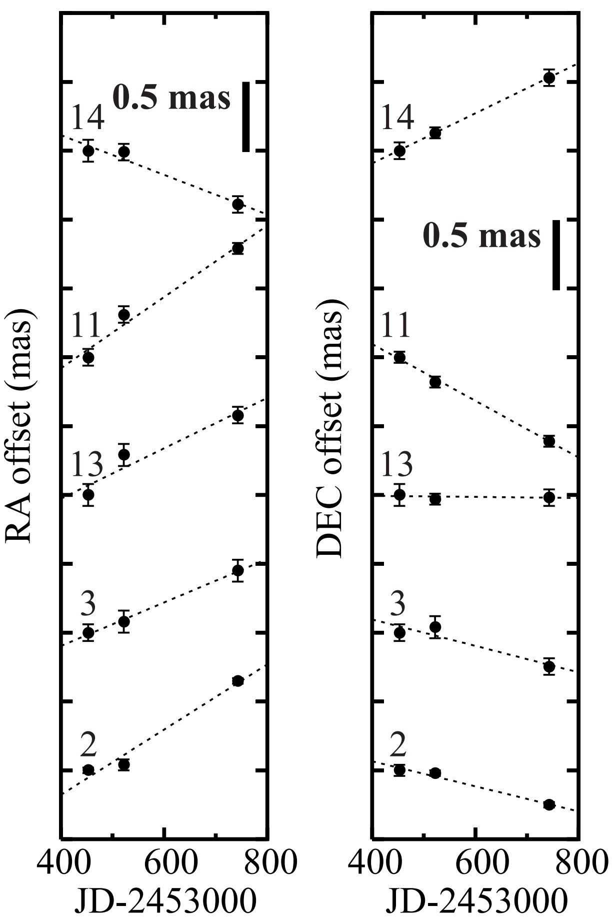

Fig. 3. Observed relative proper motions of the water-maser features in ON 1. The proper motions of only the maser features detected at all three epochs are presented. The number added for each sub-panel shows the assigned one listed in table 2. The dash line indicates a least-squares-fitted line assuming a constant-velocity motion.

($\sim$ 10 km s^{-1}). Their LSR velocities are close to the LSR velocity of the quiescent molecular cloud observed in the NH_3 line ($V_{\rm LSR} \sim 10$ km s^{-1}: Zheng et al. 1985). This may indicate an interaction between the outflow and the dense surrounding cloud (Genzel et al. 1981). Their proper motions are within $\mu_x = 0.5$–1.5, $\mu_y = -0.5$ to -0.3 mas yr^{-1}, which correspond to $V_x = 4$–13, $V_y = -4$ to -3 km s^{-1}.

The proper motion of WMC 2 shows $\mu \sim 1$ mas yr^{-1} ($V \sim 10$ km s^{-1}). Althouth it is unknown what is associated with WMC 2, the proper motions of WMC 2 did not originate from WMC 1. This indicates the presence of a driving source that is different from WMC 1. Therefore, our proper-motion measurements show that there are at least two driving sources of water masers in ON 1.

4. Discussion

4.1. Driving Sources of Water Masers

Figure 2a shows the positions of the water masers relative to the 8.4 GHz continuum emission. The water masers are located at 2″ east from the peak of the 8.4 GHz continuum emission with an absolute position accuracy of $\approx$ 0.″3 (Argon et al. 2000). The water masers are not coincident with the UC H II region, and appear to be associated with the YSO formed on the east side of the UC H II region.

Submillimeter continuum emission traces dust emission around a YSO. The 345 GHz continuum emission observed with SMA has two components of north-eastern (SMA 1) and south-western (SMA 2) ones (Su et al. 2004). The water masers would be associated with SMA 1 and SMA 2. Water masers appear to have a position offset of approximately 1″ south-east from both peak positions of the 345 GHz continuum emission. This offset would be due to an insufficient angular resolution of a 345 GHz continuum observation of $\sim$ 3″ and insufficient absolute position accuracy.

A 10.5 μm infrared source, which was not detected in the 2.2 μm and 3.75 μm emissions (Kumar et al. 2003), is situated near the center of the two WMCs and UC H II region.

Table 3. Properties of B0 star in the UC H II region and YSOs in WMC 1 and WMC 2.

No	Name	Emission	Maser	Velocity span* (km s^{-1})	Luminosity ($L_{\odot}$)	Age† (yr)	Mass‡ ($M_{\odot}$)
1 ...	B0 star	Ionized gas§ + Dust‖	OH#	~ 15#	$10^{4.2}$**	$\sim 10^5$	~ 15
2 ...	WMC 1 YSO	Dust§	Water	~ 100	$< 10^4$††	$\sim 10^4$	~ 2–15
3 ...	WMC 2 YSO	Dust‖	Water	~ 10	$< 10^4$††	...	≤ 2–15

* LSR velocity span of masers.
† Estimated ages of B0 star and WMC 1 YSO (see subsections 4.2 and 4.3).
‡ Estimated masses (see subsection 4.3).
§ Traced by 8.4 GHz continuum emission (Argon et al. 2000).
‖ Traced by 345 GHz continuum emission (Su et al. 2004).
\# Results obtaind in OH maser observation (Fish et al. 2005).
** Luminosity obtained in 1.3 to 20 cm radio continuum emissions (MacLeod et al. 1998).
†† Luminosity estimated from the far-infrared and radio continuum emissions (see subsection 4.1).

Because the 10.5 μm emission is extended in a $3'' \times 3''$ area, it is unclear whether this is associated with the present water maser features.

The total far-infrared luminosity of ON 1 derived from the IRAS data is $10^{4.1} L_{\odot}$, and the luminosity of the UC H II region observed in 1.3 to 20 cm radio continuum emission is $10^{4.2} L_{\odot}$ (MacLeod et al. 1998). The agreement of the luminosities of the far-infrared and radio continuum emissions indicates that ON 1 has a single luminous star of spectral type B0 ($L \geq 10^4 L_{\odot}$), which forms the UC H II region. The luminosities of YSOs in WMC 1 and WMC 2 seem to be lower ($< 10^4 L_{\odot}$) than that of the B0 star exciting the UC H II region.

We may thus conclude that the water masers, WMC 1 and WMC 2, are associated with two YSOs on the eastern side of UC H II region. These two YSOs are still surrounded by dusty envelopes, emitting the 345 GHz submillimeter emission.

4.2. *Outflow and YSO in WMC 1*

The outflow of WMC 1 is coincident with a jet-like outflow extended in the east–west direction by ~ 0.07 pc, which was found by IRAM observations in the ^{12}CO $J = 2$–1 line (Kumar et al. 2004). The dynamical age of CO 2–1 outflow is estimated to be (5–7) $\times 10^3$ yr using the LSR velocity difference from the systemic velocity of CO 2–1 (12 km s^{-1}) and the inclination angle of the outflow obtained by the present work ($44^{\circ} \pm 3^{\circ}$). The velocity spans in ^{12}CO $J = 1$–0 and 2–1 lines are 35 km s^{-1} and 24 km s^{-1}, respectively (Xu et al. 2006; Kumar et al. 2004). These values are smaller than the velocity span of water masers (~ 100 km s^{-1}). This may be because the size of the high-velocity outflow observed in the water masers ($< 0.''2$) is too compact to be detected with the beam of the CO 1–0 ($\sim 15''$) and CO 2–1 ($\sim 2''$) lines. The dynamical age of the CO outflow of (5–7) $\times 10^3$ yr suggests that the age of the YSO in WMC 1 is about $\sim 10^4$ yr.

Water-maser features are most likely located in shock regions, where the outflow from YSO hits ambient gases. We derived the momentum rate of the outflow in WMC 1 using the method of Torrelles et al. (2003). The momentum rate is given by

$$\dot{P}_{\mathrm{f}} = 2\Omega_{\mathrm{f}} R^2 \rho_{\mathrm{f}} V_{\mathrm{f}}^2, \tag{1}$$

where $\Omega_{\mathrm{f}} = 2\pi[1 - \cos(\theta_{\mathrm{op}}/2)]$ is the solid angle of the outflow, R the distance from the star, ρ_{f} the mass density in the outflow, V_{f} the expansion velocity of the outflow. Assuming a typical gas density necessary for water masering, $n(\mathrm{H_2}) = 10^8$ cm^{-3} (Elizur et al. 1992), the momentum rate of outflow can be estimated to be (1–2) $\times 10^{-3} M_{\odot}$ yr^{-1} km s^{-1} for the observed expansion velocity ($V_{\mathrm{f}} = 69 \pm 11$ km s^{-1}), the distance from the star ($R = 175$ AU/cos $44^{\circ} = 245$ AU), and the opening angle ($\theta_{\mathrm{op}} = 10^{\circ}$). In addition, using this momentum rate and dynamical age derived from the CO 2–1 outflow, we can estimate the momentum of the outflow in WMC 1 to be 5–14 $M_{\odot}$ km s^{-1}. This value is 10–30% of the momentum of the largest outflow in ON 1 with a size of 0.94 pc, found in the ^{12}CO $J = 1$–0 line (Xu et al. 2006). Therefore, the outflow in WMC 1 would not mainly contribute to the formation of the CO 1–0 outflow.

4.3. *Star Formation Activity of ON 1*

Dense molecular gas, which is traced in the CS $J = 5$–4 line (Shirley et al. 2003), and dust emission at 350 μm (Mueller et al. 2002), extend to the east and north side of the UC H II region. The different locations of the UC H II region, submillimeter continuum emissions, water masers, and dense molecular cloud suggest that the star-formation activity of ON 1 moves from west to east. In table 3, we summarize the possible properties of a B0 star exciting the UC H II region as well as the YSO associated with WMC 1 and WMC 2. The mass of the star in UC H II region is $\sim 15 M_{\odot}$, which is indicated by a spectral type of apploximately B0 (MacLeod et al. 1998). The mass of YSO in WMC 1 would be $\sim$2–15 $M_{\odot}$, because the momentum rate of the outflow in WMC 1 corresponds to a typical value of an intermediate-mass YSO (Shepherd 2005). The difference between WMC 1 and WMC 2 is only the expansion velocity of water masers. This velocity difference may reflect the difference of the outflow energy between WMC 1 and WMC 2. This indicates a lower power, implying a lower mass of the forming YSO in WMC 2 than in WMC 1.

Finally, we propose that the B0 star is the possible driving source of the CO 1–0 outflow. The dynamical age of the CO 1–0 outflow is estimated to be 7.3×10^4 yr at our assumed distance (Xu et al. 2006). Thus, we think that the age of the B0 star is $\sim 10^5$ yr.

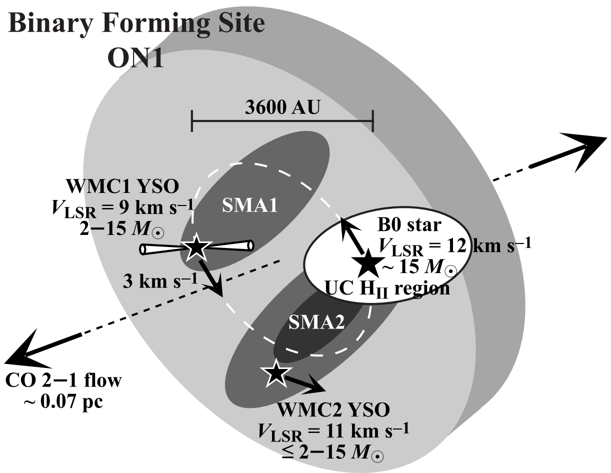

Fig. 4. Schematic representation of the structure of ON 1.

4.4. *A Binary System Formed by WMC 1 and UC H II Region?*

The LSR velocities of the WMC 1 and UC H II regions is estimated to be $V_{\rm LSR} = 9.3 \pm 6.8$, and $12.3 \pm 3.5\,\mathrm{km\,s^{-1}}$, from the systemic velocities of water masers and OH masers (Fish et al. 2005), respectively. If the WMC 1 and UC H II regions were separated at a relative velocity of $3\,\mathrm{km\,s^{-1}}$ during the formation timescale of the B0 star exciting the UC H II region of $\sim 10^5$ yr, the WMC 1 and UC H II regions should already be separaed by $\sim$60000 AU (0.30 pc). However, their separation on the sky is 3600 AU (0.017 pc). Therefore, we may consider that the WMC 1 and UC H II regions are gravitationally bound. Assuming that the WMC 1 and UC H II regions are gravitationally bound, that total mass ($M_{\rm t}$) can be estimated by

$$M_{\rm t} \sim \frac{Rv^2}{G} \tag{2}$$

$$\sim 4.1 \times \left(\frac{R}{3600\ \mathrm{AU}}\right)\left(\frac{v}{1\ \mathrm{km\ s^{-1}}}\right)^2 M_\odot, \tag{3}$$

where R is the separation of the WMC 1 and UC H II regions, and v is the relative velocity. This total mass is minimum value, because the separation along the line of sight and the relative velocity of the sky are still unknown. The total mass was derived as $M_{\rm t} \sim 37 M_\odot$ from a separation of 3600 AU and a relative velocity of $v = 3\,\mathrm{km\,s^{-1}}$. The masses of a 345 GHz dust emission core associated with the WMC 1 and UC H II regions are estimated to be 6 $M_\odot$ and 6 $M_\odot$, respectively (Su et al. 2006). Therefore, the total mass of the YSO and B0 stars, and the accompanying dust-emission cores is $\sim$ 29–42 $M_\odot$. This value is consistent with the total mass estimated on the basis the assumption of a gravitationally bound system. Therefore, we propose that the YSO in WMC 1 and the B0 star exciting the UC H II region form a binary star. The LSR velocity of WMC 2 ($V_{\rm LSR} = 11.3 \pm 2.3\,\mathrm{km\,s^{-1}}$) indicates that the YSO in WMC 2 is a third object of this bound system.

In figure 4, we illustrate a possible structure of ON 1, as inferred from the present consideration based on figure 2a. A rotating disk is found in NH_3 $(J, K) = (1, 1)$, and $H^{13}CO^+$ $J = 1$–0 lines with the VLA and the BIMA array (Zheng et al. 1985; Lim et al. 2002). The orbit shown in figure 4 is assumed to be at a position angle of 40°, which is seen in the velocity gradient in the $H^{13}CO^+$ line (Lim et al. 2002).

5. Conclusions

The following conclusions are drawn from this study:

1. We carried out three epoch observations of the ON 1 water masers with the JVN, and successfully measured the proper motions of ON 1 water masers for the first time.
2. ON 1 has two major water-maser clusters (WMC 1 and WMC 2), which are separated by 2900 AU. Both WMCs are located at 3600 AU from the UC H II region seen at 8.4 GHz continuum emission.
3. A proper-motion measurement reveals that WMC 1 is associated with a bipolar outflow elongated in the east–west direction with a high expansion velocity of $69 \pm 11\,\mathrm{km\,s^{-1}}$. This outflow is coincident with a jet-like outflow found in the CO 2–1 line.
4. WMC 1 and WMC 2 are associated with two 345 GHz continuum sources on the east side of the UC H II region. These two YSOs are still surrounded by dusty envelopes.
5. The star-formation activity of ON 1 appears to move from the west side of the UC H II region to the east side of two WMCs and a dense molecular cloud is observed in CS lines.
6. We suggests that the WMC 1 and UC H II regions in ON 1 form a binary system. The relative velocity and total mass of the WMC 1 and UC H II regions are estimated to be $\Delta V_{\rm LSR} \sim 3\,\mathrm{km\,s^{-1}}$ and $M_{\rm t} \sim 37 M_\odot$, respectively.

The authors wish to thank to all staff members and students of the VERA team for observing assistance and support. We hope VERA will observe one thousand water-maser sources in order to perform the astrometry of galactic star-forming regions, and to investigate the structure and dynamics of the Milky Way Galaxy. We thank an anonymous referee for very useful comments. T.O. and H.I. were supported by a Grant-in-Aid for Scientific Research from Japan Society for Promotion Science (17340055).

References

André, P., Ward-Thompson, D., & Barsony, M. 1993, ApJ, 406, 122
Argon, A. L., Reid, M. J., & Menten, K. M. 2000, ApJS, 129, 159
Cesaroni, R., Palagi, F., Felli, M., Catarzi, M., Comoretto, G., Di Franco, S., Giovanardi, C., & Palla, F. 1988, A&AS, 76, 445
Chikada, Y., et al. 1991, in Frontiers of VLBI, ed. H. Hirabayashi, M. Inoue, & H. Kobayashi (Tokyo: Uiversal Academy Press), 79
Doi, A., et al. 2006, PASJ, 58, 777
Downes, D., Genzel, R., Moran, J. M., Johnston, K. J., Matveyenko, L. I., Kogan, L. R., Kostenko, V. I., & Rönnäng, B. 1979, A&A, 79, 233
Elitzur, M., Hollenbach, D. J., & McKee, C. F. 1992, ApJ, 394, 221
Fish, V. L., Reid, M. J., Argon, A. L., & Zheng, X. W. 2005, ApJS, 160, 220
Genzel, R., & Downes, D. 1977, A&AS, 30, 145
Genzel, R., Reid, M. J., Moran, J. M., & Downes, D. 1981, ApJ, 244, 884
Imai, H., Kameya, O., Sasao, T., Miyoshi, M., Deguchi, S., Horiuchi, S., & Asaki, Y. 2000, ApJ, 538, 751
Imai, H., Omodaka, T., Hirota, T., Umemoto, T., Sorai, K., & Kondo, T. 2006, PASJ, 58, 883
Kumar, M. S. N., Bachiller, R., & Davis, C. J. 2002, ApJ, 576, 313
Kumar, M. S. N., Davis, C. J., & Bachiller, R. 2003, Ap&SS, 287, 191
Kumar, M. S. N., Tafalla M., & Bachiller, R. 2004, A&A, 426, 195
Kurtz, S., & Hofner, P. 2005, AJ, 130, 711
Lim, J., Choi, M., & Ho, P. T. P. 2002, ASP Conf. Ser., 267, 385
MacLeod, G. C., Scalise, E., Jr., Saedt, S., Galt, J. A., & Gaylard, M. J. 1998, AJ, 116, 1897
Moscadelli, L., Goddi, C., Cesaroni, R., Beltrán, M. T., & Furuya, R. S. 2007, A&A, 472, 867
Mueller, K. E., Shirley, Y. L., Evans, N. J., II, & Jacobson, H. R. 2002, ApJS, 143, 469
Shepherd, D. 2005, in IAU Symp. 227, ed. R. Cesaroni, M. Felli, E. Churchwell, & M. Walmsley (Cambridge: Cambridge Univ. Press), 237
Shirley, Y. L., Evans, N. J., II, Young, K. E., Knez, C., & Jaffe, D. T. 2003, ApJS, 149, 375
Su, Y. N., et al. 2004, ApJ, 616, L39
Su, Y. N., Liu, H. R., & Lim, J. 2006, in Proc. East Asian Young Astronomers Meeting 2006, ed. Y. Urata, D. Kinoshita, T. Sekiguchi, & A. Yonehara (Mitaka: National Astronomical Observatory of Japan), 17
Torrelles, J. M., et al. 2001, ApJ, 560, 853
Torrelles, J. M., et al. 2003, ApJ, 598, L115
Xu, Y., et al. 2006, AJ, 132, 20
Zheng, X. W., Ho, P. T. P., Reid, M. J., & Schneps, M. H. 1985, ApJ, 293, 522